Predicting Final Extent of Ischemic Infarction Using Artificial Neural Network Analysis of Multiparametric MRI in Patients with Stroke

H. Bagher-Ebadian, K. Jafari-Khouzani, P. D. Mitsias, H. Soltanian-Zadeh, M. Chopp, and J. R. Ewing

***Abstract*— In ischemic stroke, the pattern of recovery in brain is the most important correlate of functional recovery. Using a set of acute phase MR images (Diffusion-Weighted - DWI, T1-Weighted – T1WI, T2-Weighted T2WI, and proton density weighted - PDWI) for inputs, and the chronic T2WI at 3 months as an outcome measure, an Artificial Neural Network (ANN) was trained to predict the 3-month outcome in the form of a pixel-by-pixel forecast of the chronic T2WI. The ANN was trained and tested using 14 slices from 3 subjects using a K-Folding Cross-Validation (KFCV) method with 14 folds. The Area Under the Receiver Operator Characteristic Curve (AUROC) for 14 folds was used for training, testing and optimization of the ANN. After training and optimization, the ANN produced a map that was very well correlated ($r = 0.88$, $p < 0.0001$) with the T2WI at 3 months. To confirm that trained ANN performed well against a new dataset, 13 slices from 4 other patients were also shown to the trained ANN. The prediction made by the ANN had an excellent overall performance (AUROC = 0.82), and was very well correlated to the 3-month ischemic lesion on T2-Weighted image.**

I. Introduction

In evaluating treatment efficacy, the pattern of recovery in brain tissue is considered to be the most important surrogate marker [1]. Consequently, during the acute phase of ischemic stroke, a fast and reliable identification of ischemic tissue, and a prediction as to its fate, would aid clinical decision-making, helping to maximize benefit and minimize side effects of a therapeutic intervention [2, 3]. Many studies, by correlating with follow-up imaging or neurological status, have shown the potential for diffusion weighted imaging (DWI), perfusion weighted imaging (PWI), and/or T2-weighted (T2WI) magnetic resonance imaging (MRI) used together for staging stroke outcome [4-6]. Most of these analyses were performed using as an outcome metric the volume of a region-of-interest (ROI) defined by the difference between an acute data set and the outcome image [6-8]. For instance, it has been shown that unsupervised clustering approaches, such as the ISODATA (Iterative Self-Organizing Data Analysis) Technique can utilize combined MRI data sets from the acute [9, 10] and the subacute [1] phase post-stroke to predict final infarct volume and thus produce a time-independent surrogate MRI outcome predictor [2, 10-13]. However ISODATA has some significant drawbacks.

ISODATA is an unsupervised segmentation procedure, related to the K-means algorithm, in the N-dimensional feature space of the combined data set. Based on the position of each pixel in the N-dimensional feature space, the algorithm assigns a membership number. In stroke, there are a few (always 12 or less) memberships, corresponding to at most 12 clusters in the N-dimensional feature space. Thus, maps produced in ISODATA are sharply delineated, and not approximately continuous as in the outcome measure, the T2WI. An associated classification scheme standardizes ISODATA clusters on the basis of two known clusters: normal white matter and CSF. For comparison purposes, signature 1 is assigned to normal white matter and signature 12 to CSF. A line in feature space connects the two clusters, and the positions of the other clusters are projected onto this line. The cluster whose projection is adjacent to 1 is assigned signature number 2, the cluster adjacent to 2 is assigned number 3, and so on. Thus, the mapping of clusters to signature numbers is to an extent arbitrary and also nonlinear in that a signature of 6 does not mean that this cluster projects twice as far along the line as does a signature of 3. This discrete and nonlinear mapping complicates potential analyses that might produce a voxel-by-voxel correlation between ISODATA as a potential surrogate measure and the T2WI outcome measure. Furthermore, to a large extent, ISODATA mapping and standardization does not produce an easily visualized association between it and the outcome measure. Additional problems in the ISODATA technique include: ISODATA's instability in the presence of image artifacts and noise, its sensitivity to initial conditions, uncertainty as to the underlying variances of the clusters, and its dependence on the assumption of normality for the distribution of clustered data [14]. Thus, ISODATA and related approaches, while useful, do not provide a pixel-by-pixel judgment as to the potential of eventual infarction; finding a continuous predictor for infarction remains an open problem [15, 16] The ANN approach herein proposed corrects many of the deficiencies of clustering approaches. It provides a very fast (essentially real-time), approximately continuous, and intuitive mapping of the predicted outcome, while preserving the time-independent and multi-parametric

Manuscript received January 5, 2009. This work was supported in part by Grant NIH R03NS061170 (NINDS). James R. Ewing is with Department of Neurology, Henry Ford Hospital, Detroit, MI 48202 (Phone: 313-916-2620, Fax: 313-916-1324, jre@neurnis.neuro.hfh.edu). He is also with Department of Physics Oakland University, Rochester, MI 48309 and Department of Physiology and Neurology, Wayne State University, Detroit, MI 48202. Hassan Bagher-Ebadian is with Department of Neurology, Henry Ford Hospital, Detroit, MI 48202 USA. Hassan Bagher-Ebadian is also with Department of Physics, Oakland University, Rochester, MI 48309. Kourosh Jafai-Khouzani and Hamid Soltanian-Zadeh are with Department of Diagnostic Radiology, Henry Ford Hospital, Detroit, MI 48202. Panayiotis D. Mitsias and Michael Chopp are with Department of Neurology, Henry Ford Hospital, Detroit, MI 48202.

strengths of the ISODATA approach.

II. Materials and Methods

A. Hypothesis

We hypothesized that, given a T2 weighted image at the chronic stage of stroke (3 months post-stroke), an ANN might be trained to directly predict the size and pattern of the tissue recovery from the information available in acute phase MR images.

B. Patients and MRI Studies

An acute phase MRI image set consisting of a T1-weighted (T1WI), T2WI, DWI and proton density (PDWI) was selected as the input set to the ANN. The co-registered three month T2 weighted image, considered to be the gold standard for final infarct size (and estimation of the tissue recovery), was employed as the training set. Seven patients (27 total slices) with acute neurological deficit consistent with ischemic stroke, and MRI studies within 24 hours of onset (defined as the last time the patient was known to be without neurological deficit), were selected. Of this set of seven patients, three with the best quality images (14 total slices) were used for training an ANN. The severity of neurological deficit was assessed at the time of the MRI study using the National Institutes of Health Stroke Scale (NIHSS) score [1-3, 5]. MRI studies were performed at the acute time point (<24 h post-ictus), and at outcome (3 months post-ictus). Patients with cerebral hemorrhage or a history of prior stroke were excluded.

MRI studies were conducted on a 1.5-tesla GE Signa MR scanner with echo-planar capability (GE, Milwaukee, WI). Each MRI study consisted of axial multispin echo T2WI, and DWI with slice thickness 6 mm. The field of view (FOV) was 240 X 240 mm. For T1WI and T2WI, the matrix was 256 X 192 and for DWI 128 X 128. Additional parameters for each study were: (a) T1WI: TR/TE = 600/14 ms; (b) T2WI: TR/TE = 2,800/30, 60, 90, 120 ms; (c) axial DWI was performed using an echo-planar sequence, TR/TE = 10,000/101 ms, b-values = 1,000, 600, 300, 0 s/mm2, 1 NEX.

For each patient, four image sets (T1WI, T2WI, DWI and PDWI) at the acute time point were selected to provide input features to the ANN. All acute- and chronic phase images were registered to the acute T2WI using Eigentool software [17]. To reduce mis-registration effects, images were smoothed using a unity filter with a 3X3 window, and then normalized to their mean value, thus creating a feature set insensitive to the MR system gain. ROIs were defined by thresholding the 3-month T2WI to outline the region of infarction. This region was reflected around the midline and adjusted so that the resultant region selected a visually normal contralateral area of tissue, so as to approximately balance normal and infarcted tissue (prevalence~ 0.35). The selected infarcted and normal regions were used together as inputs to the ANN.

C. Inputs and Training Set for the ANN

Using the normalized data from the selected ROIs, a feature set was generated from the four selected acute-phase images and presented to a feed-forward multilayer perceptron (MLP) with back propagation training algorithm as an input vector. In this type of ANN, as shown in Fig. 1, the nodes are organized in the input layer, hidden layers, and the output layer. Nodes are interconnected by weights in such a way that information propagates from one layer to the next through a sigmoid (bipolar) activation function. Learning rate and momentum factors control the internode weight adjustment during the training. A back propagation learning strategy [18-20] was employed for training the ANN in a supervised mode. In this strategy, a trial set of weights (the weight vectors, one vector for each layer of the ANN) is

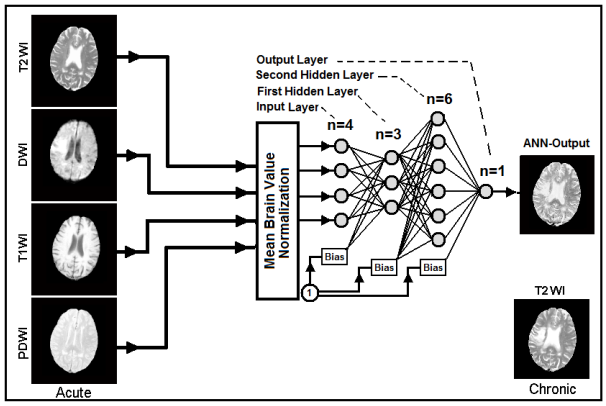

Fig. 1. ANN diagram for phase of training and prediction. As shown in this figure, 4 MR image modalities are input to the ANN to predict T2WI at three month. Note that the MR modalities are normalized to their brain mean values before feeding to the ANN.

proposed. The input vectors are presented to the ANN, and the output result compared to the class identifier (in our case, this was the co-registered T2 weighted image at three month study). The weight vectors are then adjusted to minimize some measure of error, i.e., the Mean Square Error (MSE) between the output of the ANN and the training set. This procedure is performed iteratively across the entire data set.

Batch processing was used to improve the convergence rate and the stability of training. The weight changes obtained from each training case were accumulated, and the weights updated after the entire set of training cases was evaluated. Batch processing improves stability, but with a tradeoff in the convergence rate [20, 21]. A K-fold cross-validation (KFCV) method was employed for training, testing, and network optimization [21, 22].

D. ANN Optimization and Generalization Error

To generalize the ANN, i.e., to allow its application to a wide range of inputs, we needed to avoid both under-fitting of the training data (which generates a high variance in the output estimate) and over-fitting of the training data (which produces biased outputs). There are a number of strategies for assuring generalization:

1. Optimize the number of free parameters (independent connection weights) in the model (e.g., the number of neurons in each layer and the number of layers). 2. Stop the gradient descent training at an appropriate point. 3. Add noise to the training patterns to smooth out the data points. Strategy number 3 is employed in cases where local minima "trap" the ANN optimization process. Since no trapping was observed, strategy number 3 was not employed in this study. To employ strategies number 1 and 2, we must estimate from

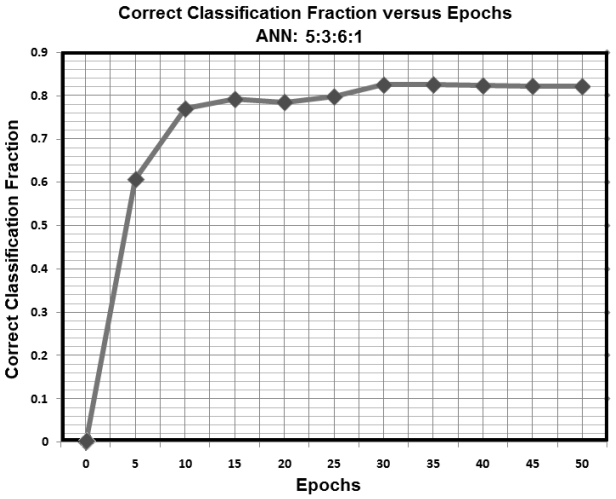

Fig. 2. Correct Classification Fraction versus epochs in training and testing phases for the optimal ANN (4:3:6:1) using 14 slices of three patients with 14 folds. Note the termination epoch is around 35, which is corresponded to 10% of CCF curve plateau.

our training data what the generalization error is likely be.

A K-fold cross-validation (KFCV) method was employed for training, testing, and network optimization [20-23]. To characterize the generalization error, we trained and validated the ANN by the KFCV method using the area under the receiver operating curve (AUROC) as a cost function [21, 22, 24, 25]. In KFCV, the training data are divided at random into K distinct subsets, the network is then trained using K–1 subsets, and tested on the remaining subset. The process of training and testing is then repeated for each of the K possible choices of the subset omitted from the training. In our case, a large number (n=50) of the random subsets were used for training and cross-validation. The average Correct Classification Fraction (CCF) at different epochs for the K omitted subsets was plotted and the epoch corresponding to 10% of its plateau was taken to be the stopping epoch. The mean squared error (MSE) of the ANN for all K subsets at the different epochs was calculated and its average value at the stopping epoch was taken as the measure of generalization error. This procedure has the advantage that it allows us to use a high proportion of

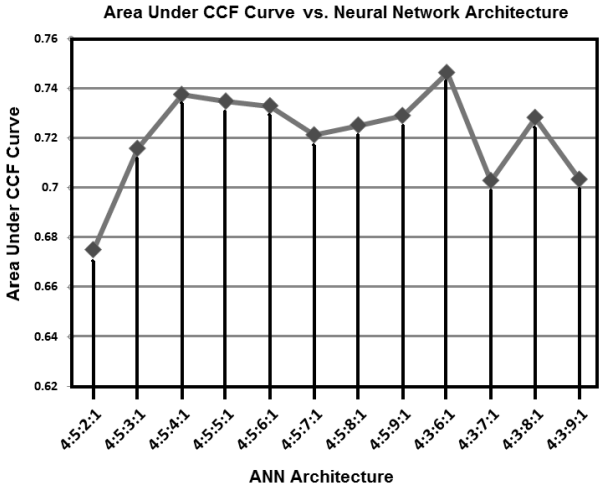

Fig. 3. Area Under Correct Classification Fraction (AUCCF) curve versus number of neurons in the second hidden layer. As shown in this figure, AUCCF is maximum for six neurons in the second hidden layer.

the available training data, a fraction (1 – 1/K), for training, while making use of all the data points in estimating the generalization error or agreement.

The cost is that the process can be lengthy, since we need to train and evaluate the network K times. Typically, K≈10 is considered reasonable [22, 25]. In this study, K was set to 14 for 14 slices of 3 patients (1 in each fold) and the ANN had a single output, to predict a T2WI at the chronic time point.

To measure how accurately this ANN matched the whole input dataset (each set of MR modalities for all pixels) with the entire outcome set (each pixel in all 3-month T2 studies), as shown in Fig. 2, the ANN's Correct Classification Fraction (CCF) curve was generated at different levels of epochs during the KFCV procedure. The Area Under Correct Classification Fraction (AUCCF) which is proportional to AUROC (Az) value, was used as an index to compare the ANN's performance, to determine the optimal architecture of the ANN, and to find the ANN termination error [25, 26]. Each KFCV set was trained until its error was below a defined termination error (i.e., the point at which the training procedure was stopped). The termination error was set by determining the error at the 10% point of the CCF's plateau.

The number of hidden layer nodes may affect the performance of the ANN classifier [22, 24]. Since the ANN could not be trained by less than 3 neurons in its first hidden layer, layer and node optimization were done by maximizing

the AUCCF value for its second hidden layer as a function of the number of nodes.

Internally, in the ANN, the activation function of the ANN neurons is a sigmoid function that is most easily programmed to work in a polar mode between –1 and 1; the one output neuron has a saturated function (uni-polar) with a range 0 to 1.0. In order to present an easily understood comparison, the response of the trained ANN was compared to the chronic T2WI (gold standard) by calculating a correlation coefficient using all of the pixel comparisons available and ROC curve of the optimal ANN. Finally, the optimized ANN was used to predict the T2 weighted image of outcome in the 4 patients (13 slices) that had not been included in the training set (KFCV).

III. Results

Training and validation objectives of the ANN were accomplished in the KFCV method. To test the performance of the trained ANN against a new dataset, a total of 13 slices of acute data taken in an additional 4 patients was used to further test the trained ANN. As in Fig. 1, a set of 4 feature vectors extracted from DWI, T1WI, T2WI and PDWI were presented to the ANN and the performance of the ANN with respect to its number of second hidden layer nodes was examined by considering the AUCCF value at a KFCV termination error (MSE) of (MSE=0.012 ~ 35 epochs). The ANN was trained and tested for a set of normal and lesion ROIs. For a statistically reliable comparison, and to increase the ANN's accuracy for lesion detection, map sampling was done at a prevalence of about 0.35 by choosing regions of interest (ROIs) from normal tissue at about half the area of the lesion area.

The optimal ANN ([4+1 bias]:[3+1 bias]:[6 +1 bias],[1]) was found by maximization of the AUCCF value for 2 hidden layers. In Fig. 2, a plot of the CCF curve (for the optimal ANN; 4:3:6:1) and in Fig. 3 the AUCCF vs. the number of neurons in the second hidden layer for a stopping error of 0.012, learning rate of 0.01 and momentum of 0, are shown. As Fig. 3 demonstrates, the maximum value of the AUCCF (~0.75) gives the optimal number of neurons (six neurons plus one bias) in the second hidden layer.

Using all 7 patients (27 slices), the trained ANN ([4+1 bias]:[3+1 bias]:[6 +1 bias],[1]) generated maps that were well correlated (r=0.88, p<0.0001) with the chronic T2WI. Fig. 4 contains six exemplary results, showing the acute DWI study (left-hand column), the chronic T2WI (middle column), and the ANN outcome predicted by the acute image set (right-hand column). Image sets 1 through 4 were members of the training set, while image sets 5 and 6 were not members of the training set (selected from 4 patients who were not in the training set).

As Fig. 4 demonstrates, the ANN's predictions, generated in seconds by the trained ANN, are visually similar to their corresponding chronic T2 weighted images; the pattern and lesion size predicted by the ANN are pretty well matched with their three-month lesion in both training and test examples. Note that the continuity of the ANN output provides more information regarding the tissue viability compared to other statistical techniques such as ISODATA.

Fig. 5 presents the scatter plot of the ANN response versus T2–weighted image at three months for lesion (gray dots) and control areas (black dots) for all 27 slices of seven patients. As previously note, the ANN prediction for all 27 slices of seven patients was highly correlated (r=0.88, p <

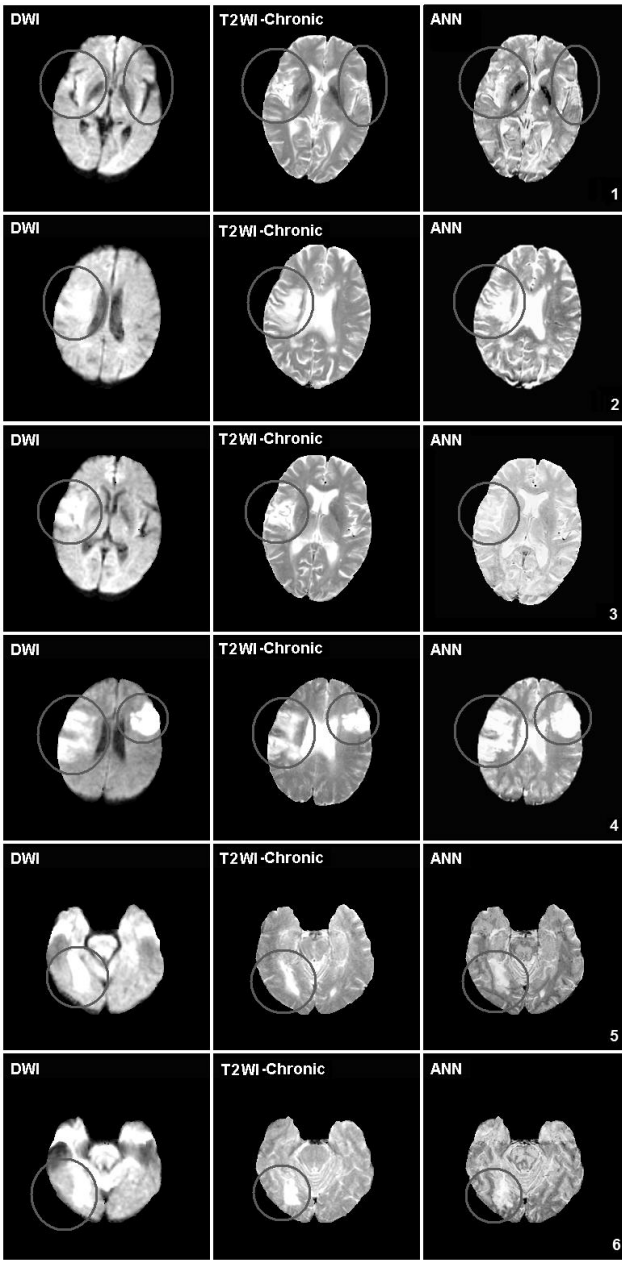

Fig. 4. Examples of ANN-produced images in 6 exemplary MRI slices. Left column: DWI in acute study. Middle: outcome T2WI. Right: ANN predicted outcome from acute image set. Image sets 1, 2, 3, and 4 were members of the training set. Image sets 5 and 6 were not members of the training set.

0.0001) with the T2WI outcome measure at three month. The AUROC, which represents the performance of the trained ANN, was 0.82 for the combined dataset. When the trained ANN was tested on the 13 slices of data from the 4 patients not used for training the correlation coefficient was 0.77, $p < 0.0001$. To estimate the overall performance of the trained ANN, ROC curve of the trained ANN (4:3:6:1) was generated for all training samples and the Area Under ROC (AUROC=0.82) was considered as the performance of the trained ANN (see Fig. 6). As shown in Fig. 6, the optimal sensitivity and specificity of the ANN were calculated at the half angle and ROC curve intercept point (Specificity Optimal =0.71, Sensitivity Optimal=0.73) which implies that the ANN can predict the lesions with sensitivity of 73% at a specificity of the 71%. Fig. 7 compares the results of ISODATA technique with ANN. As shown in this figure, the lesion area in ISODATA map is clustered to three different signatures (6, 7, and 12). Signatures range between one (corresponding to normal tissue) to twelve (corresponding to CSF or dead tissue). Whereas the ANN demonstrates a continuous map for the status of the tissue at risk in the lesion area, the ISODATA only shows three possibilities (6, 7, and 12) corresponding to the chance of tissue recovery after three months. However, both techniques are in agreement in the CSF area or dead tissue.

IV. Discussion

An ANN was trained and tested to directly predict the size and pattern of the eventual tissue damage from the information available in acute phase MR images using T2 weighted image at the chronic stage of stroke (3 months post-stroke) as a gold standard of training. The results indicate that a trained ANN is capable of predicting the pattern and size of eventual infarction, using MR acute information. Since it provides a visual estimate of the outcome, such modeling may play an important role in the assessment of therapeutic interventions applied within extended therapeutic windows, currently of great interest in the treatment of stroke. It must be noted that the training set was quite small in the number of patients and images (14 slices of 3 patients); that is why the KFCV method was used for training and evaluation.

It was kept small so that we could examine different tactics for the construction of the ANN, and get a result in a reasonable amount of time. A best-quality subset of images

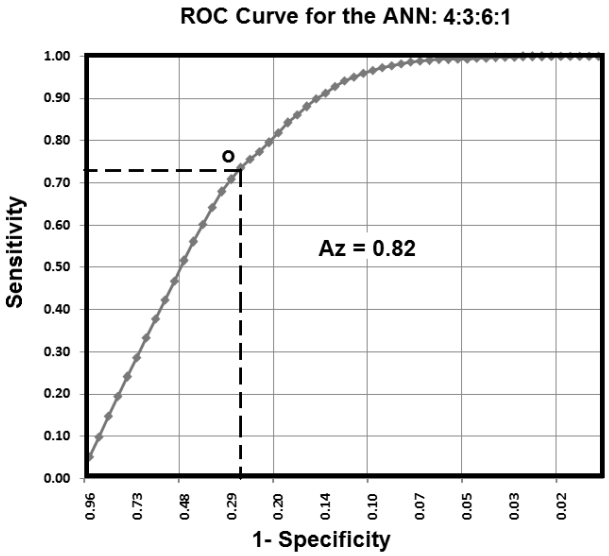

Fig. 6. ROC curve (AUROC=0.82) for the trained ANN (4:3:6:1). As shown in this Figure, the optimal sensitivity and specificity of the ANN are calculated at the half angle and ROC curve intercept point (Point O; Specificity Optimal =0.71, Sensitivity Optimal=0.73) which implies that the ANN can predict lesion and tissue with a sensitivity of 73% and a specificity of the 71%.

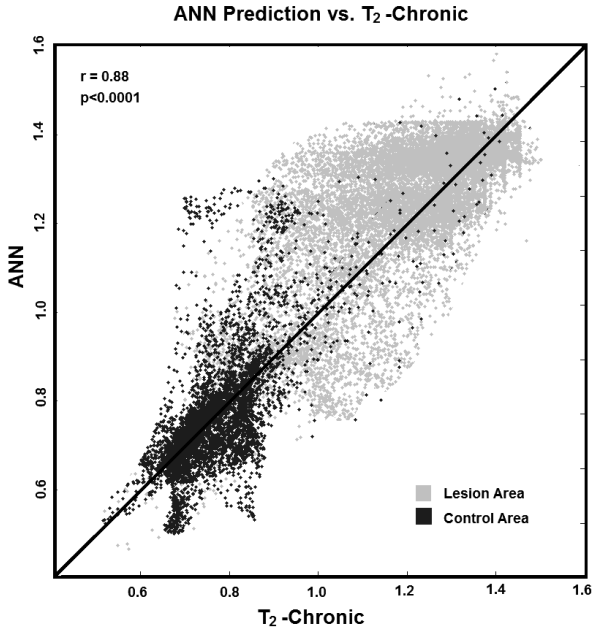

Fig. 5. Scatter plot of the optimized ANN (4:3:6:1) for predicting lesion and normal areas (gray and black dots respectively) of 27 slices in 7 patients compare to their T2WI at chronic (gold standard). As shown in this figure, the ANN prediction is highly correlated (N=470266, t=1024.47, df(N-2)=470264, r=0.88, p-one-tailed=p-two-tailed=0.0001) with the T2WI at three month.

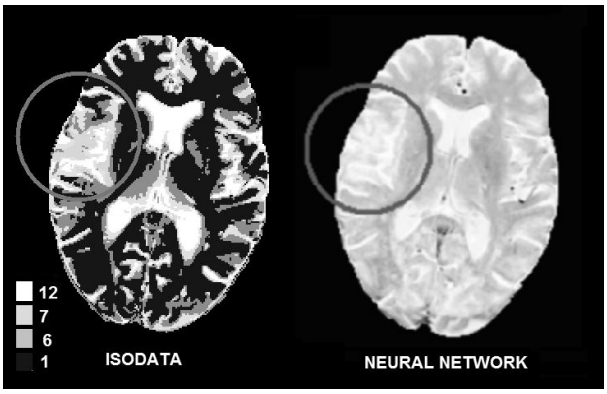

Fig. 7. Circles in both maps (ISODATA and ANN) denotes the lesion area. In ISODATA the lesion is clustered into three different signatures (12, 7, and 6). Signature number indicates the chance of tissue recovery. The higher the signature values, the higher the chance of recovery.

was selected to guard against the danger of biasing the ANN with low-quality images. However, when the image sets that were not included in the training set were submitted to the ANN, the predicted outcome was visually in good agreement with the 3-month T2WI lesion size (Fig. 4) and had a high correlation coefficient. This demonstrates that an ANN constructed using even a relatively restricted set of data, when tested on a different (and, as far as we could judge, inferior) input data set, continued to produce a robust estimate of outcome. Note that the selection of the infarct and balancing information from normal regions (There were nearly twice as many infarct samples as normal samples; prevalence ~ 0.35), slants the accuracy of the ANN toward detection of the lesion recovery. Even this small pilot study demonstrates a robust and sensitive predictor of infarct outcome, and because it can be produced almost in real-time as the image sets emerge from the MRI, shows great potential as a tool that may eventually influence clinical practice.

For future study, we expect to construct an ANN predictor of outcome T2WI that is essentially time-independent, either because the acute/subacute T2WI image, with its increasing contrast with time post-ictus, itself provides a kind of biological clock that measures the post-stroke duration, or by entering time post-ictus as one of the input parameters to the ANN. Clinical neurological recovery, as measured by the change in NIHSS, can also be used as additional information for training the ANN in acute to chronic time point (30). Therefore, it may be possible to form a more clinically relevant prediction of outcome by including the NIHSS score as an input to the ANN, in addition to the stated feature set.

A fast, robust, and time-independent predictor of stroke outcome raises the possibility of real-time evaluation of stroke in progress, acute stroke and subacute stroke. Given effective treatments, a real-time predictor of outcome can produce a paradigm shift in the treatment of stroke in all its early stages, and may ameliorate or avoid many of the profoundly destructive sequelae of cerebral infarction.

ACKNOWLEDGMENT

This study is supported in part by Grant NIH R03NS061170 (NINDS). The authors would like to thank Dr. Ramesh Paudyal form Neurology Department and Dr. David Hearshen and his staff from department of Radiology for their invaluable helps in data retrieving.

REFERENCES

[1] P. D. Mitsias, J.R. Ewing, M. Lu, M. Pasnoor, H. Bagher-Ebadian, Q.M. Zhao, S. Santhakumar, M.A. Jacobs, N.I.H. Papamitsakis, H. Soltanian-Zadeh, D.O. Hearshen, S.C. Patel, M. Chopp, "Multiparametric Iterative Self-Organizing MR Imaging Data Analysis Technique for Assessment of Tissue Viability in Acute Cerebral Ischemia," *American Journal of Neuroradiology*, vol. 25, pp. 1499- 1508, 2004.

[2] P. D. Mitsias, J.R. Ewing, M. Lu, M. Pasnoor, H. Bagher-Ebadian, Q.M. Zhao, S. Daley, H. Soltanian-Zadeh, M. Chopp, "Emergency administration of abciximab for treatment of patients with acute ischemic stroke: results of a randomized phase 2 trial," *Stroke*, vol. 36, pp. 880-90, Apr 2005.

[3] G. W. Albers, "Expanding the window for thrombolytic therapy in acute stroke. The potential role of acute MRI for patient selection," *Stroke*, vol. 30, pp. 2230-7, Oct 1999.

[4] C. Oppenheim, C. Grandin, Y. Samson, A. Smith, T. Duprez, C. Marsault, and G. Cosnard, "Is there an apparent diffusion coefficient threshold in predicting tissue viability in hyperacute stroke?," *Stroke*, vol. 32, pp. 2486-91, Nov 2001.

[5] J. F. Arenillas, A. Rovira, C. A. Molina, E. Grive, J. Montaner, and J. Alvarez-Sabin, "Prediction of early neurological deterioration using diffusion- and perfusion-weighted imaging in hyperacute middle cerebral artery ischemic stroke," *Stroke*, vol. 33, pp. 2197-203, Sep 2002.

[6] P. D. Mitsias, M. A. Jacobs, R. Hammoud, M. Pasnoor, S. Santhakumar, N. I. Papamitsakis, H. Soltanian-Zadeh, M. Lu, M. Chopp, and S. C. Patel, "Multiparametric MRI ISODATA ischemic lesion analysis: correlation with the clinical neurological deficit and single-parameter MRI techniques," *Stroke*, vol. 33, pp. 2839-44, Dec 2002.

[7] P. W. Schaefer, G. J. Hunter, J. He, L. M. Hamberg, A. G. Sorensen, L. H. Schwamm, W. J. Koroshetz, and R. G. Gonzalez, "Predicting cerebral ischemic infarct volume with diffusion and perfusion MR imaging," *AJNR Am J Neuroradiol*, vol. 23, pp. 1785-94, Nov-Dec 2002.

[8] A. E. Baird, A. Benfield, G. Schlaug, B. Siewert, K. O. Lovblad, R. R. Edelman, and S. Warach, "Enlargement of human cerebral ischemic lesion volumes measured by diffusion-weighted magnetic resonance imaging," *Ann Neurol*, vol. 41, pp. 581-9, May 1997.

[9] G. Montalescot, P. Barragan, O. Wittenberg, P. Ecollan, S. Elhadad, P. Villain, J. M. Boulenc, M. C. Morice, L. Maillard, M. Pansieri, R. Choussat, and P. Pinton, "Platelet glycoprotein IIb/IIIa inhibition with coronary stenting for acute myocardial infarction," *N Engl J Med*, vol. 344, pp. 1895-903, Jun 21 2001.

[10] P. D. Mitsias, J.R. Ewing, M. Lu, H. Bagher-Ebadian, Q.M. Zhao, H. Soltanian-Zadeh, M. Chopp, "Abciximab in acute ischemic stroke: a randomized, double-blind, placebo-controlled, dose-escalation study. The Abciximab in Ischemic Stroke Investigators," *Stroke*, vol. 31, pp. 601-9, Mar 2000.

[11] B. Eckert, C. Koch, G. Thomalla, T. Kucinski, U. Grzyska, J. Roether, K. Alfke, O. Jansen, and H. Zeumer, "Aggressive therapy with intravenous abciximab and intra-arterial rtPA and additional PTA/stenting improves clinical outcome in acute vertebrobasilar occlusion: combined local fibrinolysis and intravenous abciximab in acute vertebrobasilar stroke treatment (FAST): results of a multicenter study," *Stroke*, vol. 36, pp. 1160-5, Jun 2005.

[12] N. M. Menezes, H. Ay, M. Wang Zhu, C. J. Lopez, A. B. Singhal, J. O. Karonen, H. J. Aronen, Y. Liu, J. Nuutinen, W. J. Koroshetz, and A. G. Sorensen, "The real estate factor: quantifying the impact of infarct location on stroke severity," *Stroke*, vol. 38, pp. 194-7, Jan 2007.

[13] K. S. Butcher, M. Parsons, L. MacGregor, P. A. Barber, J. Chalk, C. Bladin, C. Levi, T. Kimber, D. Schultz, J. Fink, B. Tress, G. Donnan, and S. Davis, "Refining the perfusion-diffusion mismatch hypothesis," *Stroke*, vol. 36, pp. 1153-9, Jun 2005.

[14] M. Koga, D. C. Reutens, P. Wright, T. Phan, R. Markus, B. Pedreira, G. Fitt, I. Lim, and G. A. Donnan, "The existence and evolution of diffusion-perfusion mismatched tissue in white and gray matter after acute stroke," *Stroke*, vol. 36, pp. 2132-7, Oct 2005.

[15] M. A. Jacobs, P. Mitsias, H. Soltanian-Zadeh, S. Santhakumar, A. Ghanei, R. Hammond, D. J. Peck, M. Chopp, and S. Patel, "Multiparametric MRI tissue characterization in clinical stroke with correlation to clinical outcome: part 2," *Stroke*, vol. 32, pp. 950-7, Apr 2001.

[16] H. Soltanian-Zadeh, H. Bagher-Ebadian, J. R. Ewing, P. D. Mitsias, A. Kapke, M. Lu, Q. Jiang, S. C. Patel, and M. Chopp, "Multiparametric iterative self-organizing data analysis of ischemic lesions using pre- or post-Gd T1 MRI," *Cerebrovasc Dis*, vol. 23, pp. 91-102, 2007.

[17] J. P. Windham, M. A. Abd-Allah, D. A. Reimann, J. W. Froelich, and A. M. Haggar, "Eigenimage filtering in MR imaging," *J Comput Assist Tomogr*, vol. 12, pp. 1-9, Jan-Feb 1988.

[18] W. S. McCulloch and W. Pitts, "A logical calculus of the ideas immanent in nervous activity. 1943," *Bull Math Biol*, vol. 52, pp. 99-115; discussion 73-97, 1990.

[19] K. Gurney, *An Introduction to Neural Networks* vol. 1. London: Routlege, 1997.

[20] J. Freeman and D. Skapura, *Neural Network-Algorithms, Applications and Programming Techniques* vol. 1. Reading, MA: Addison-Wesley, 1991.

[21] C. Looney, *Pattern recognition using neural networks: theory and algorithms for engineers and scientists* vol. 1. New York: Oxford University Press, 1997.

[22] C. Bishop, *Neural Networks for Pattern Recognition* vol. 1. London-United Kingdom: Oxford University Press, 1997.

[23] H. Bagher-Ebadian, H. Soltanian-Zadeh, S. Seayeshi, and S. T. Smith, "Neural Network and Fuzzy Clustering Approach for Automatic Diagnosis of Coronary Artery Disease in Nuclear Medicine," *IEEE Transactions on Nuclear Science*, vol. 51, pp. 184-192, 2004.

[24] H. Bagher-Ebadian, T. N. Nagaraja, R. Paudyal, P. Whitton, S. Panda, J. D. Fenstermacher, and J. R. Ewing, "MRI estimation of contrast agent concentration in tissue using a neural network approach," *Magn Reson Med*, vol. 58, pp. 290-7, Aug 2007.

[25] M. E. Hosseini-Ashrafi, H. Bagherebadian, and E. Yahaqi, "Pre-optimization of radiotherapy treatment planning: an artificial neural network classification aided technique," *Phys Med Biol*, vol. 44, pp. 1513-28, Jun 1999.

[26] J. L. Luby M, Jose´ GM, Bykowski JL, Bethesda MD, Schellinger PD, Warach S., " Neural Network Model for Prediction of Final Infarct Volume in Treated versus Untreated Stroke Patients," *Storke-Neurologische Klinik*, vol. 39 Erlangen, Germany, p. 588, 2008.